Electronic Supplementary Material (ESI) for RSC Advances.
This journal is © The Royal Society of Chemistry 2016

Electronic Supplementary Information for:

Iodine-Selective RedOx-Active Hydrotalcite Composites

Tatiana G. Levitskaia,[a]* Sayandev Chatterjee,[a] Bruce W. Arey,[a] Emily L. Campbell,[a] Yongchun Hong,[b] Libor Kovarik,[b] James M. Peterson, [a] Natasha K. Pence, [a] Jesus Romero,[a] Vaithialingam Shutthanandan,[b] Birgit Schwenzer[c] and Tamas Varga[b]

[a] Energy and Environment Directorate, Pacific Northwest National Laboratory, Richland, WA 99354, United States.
[b] Environmental and Molecular Sciences Laboratory, Pacific Northwest National Laboratory, Richland, WA 99354, United States.
[c] Physical and Computational Sciences Directorate, Pacific Northwest National Laboratory, Richland, WA 99354, United States.

Table of Contents

Title	Page No.
Table S1. Concentrations of the selected specified constituents in the groundwater collected from U.S. Department of Energy Hanford Site (200 area, well 299-W19-36).	S3
Table S2. Assignment of XPS peaks.	S4
Table S3. Elemental analysis of the marked regions in Figure S2 for the untreated **Co-Cr** and **Ni-Cr** composites obtained from EDS analyses showing the respective atomic percentages of the elements.	S5
Table S4. Elemental analysis of the marked regions in Figure S4 for the IO_4^- treated **Co-Cr** composite obtained from EDS analyses showing the respective atomic percentages of the elements.	S5
Table S5. Elemental analysis of the marked regions in Figure S6 for the IO_3^- treated **Co-Cr** composite obtained from EDS analyses showing the respective atomic percentages of the elements.	S6
Table S6. Elemental analysis of the marked regions in Figure S8 for the I^- treated **Co-Cr** composite obtained from EDS analyses showing the respective atomic percentages of the elements.	S6
Table S7. Elemental analysis of the marked regions in Figure S10 for the IO_4^- treated **Ni-Cr** composite obtained from EDS analyses showing the respective atomic percentages of the elements.	S7
Table S8. Elemental analysis of the marked regions in Figure S11 for the IO_3^- treated **Ni-Cr** composite obtained from EDS analyses showing the respective atomic percentages of the elements.	S7
Table S9. Elemental analysis of the marked regions in Figure S12 for the I^- treated **Ni-Cr** composite obtained from EDS analyses showing the respective atomic percentages of the elements.	S7
Figure S1. XPS patterns of (—) unexposed composites, and exposed to (—) 10^{-1} M I^-, (—) IO_3^- and (—) IO_4^- for 24 hours: O 1s region for (A) **Co-Cr**, (B) **Ni-Cr**.	S8
Figure S2. Representative elemental distribution in the untreated composites: (A) Representative SEM of **Co-Cr** composite, (B) Cr mapping of the represented region (C) Co mapping for the represented region, (D) Representative SEM of **Ni-Cr** composite, (E) Cr mapping of the represented region (F) Co mapping for the represented region.	S8

Figure S3. Representative SEM images of the composites: after 7 day exposure to aqueous solutions of anions: (A) **Co-Cr** exposed to 10^{-1} M IO_4^-, (B) **Co-Cr** exposed to 10^{-1} M IO_3^-, (C) **Co-Cr** exposed to 10^{-1} M I^-, (D) **Ni-Cr** exposed to 10^{-1} M IO_4^-, (E) **Ni-Cr** exposed to 10^{-1} M IO_3^-, (F) **Ni-Cr** exposed to 10^{-1} M I^-.	S9
Figure S4. Representative elemental distribution in the IO_4^- treated **Co-Cr** composite: (A) Representative SEM image of the **Co-Cr** composite after being exposed to 10^{-1} M IO_4^- for 24 hours, (B, C, D) Co, Cr and I mapping for region represented by pane A, (E) Representative SEM image of the **Co-Cr** composite after being exposed to 10^{-1} M IO_4^- for 7 days, (F, G, H) Co, Cr and I mapping for region represented by pane E.	S9
Figure S5. (A, B) Representative TEM image of **Co-Cr** composite after exposure to 10^{-1} M IO_4^- for 24 hours (C, D) the EDS analysis of regions marked 1 and 2 respectively in pane B.	S10
Figure S6. Representative elemental distribution in the IO_3^- treated **Co-Cr** composite: (A) Representative SEM image of the **Co-Cr** composite after being exposed to 10^{-1} M IO_4^- for 24 hours, (B, C, D) Co, Cr and I mapping for region represented by pane A, (E) Representative SEM image of the **Co-Cr** composite after being exposed to 10^{-1} M IO_3^- for 7 days, (F, G, H)	S10
Figure S7. (A, B) Representative TEM image of **Co-Cr** composite after exposure to 10^{-1} M IO_3^- for 24 hours (C, D) the EDS analysis of regions marked 1 and 2 respectively in pane B.	S11
Figure S8. Representative elemental distribution in the I^- treated **Co-Cr** composite: (A) Representative SEM image of the **Co-Cr** composite after being exposed to 10^{-1} M I^- for 24 hours, (B, C, D) Co, Cr and I mapping for region represented by pane A, (E) Representative SEM image of the **Co-Cr** composite after being exposed to 10^{-1} M I^- for 7 days, (F, G, H) Co, Cr and I mapping for region represented by pane E.	S11
Figure S9. Co-Cr composite exposed to 10^{-1} M I^- for 24 hours: representative TEM images of the spinels (A) embedded in the heterogeneous matrix and (B) the magnified spinels, (C) representative TEM of the heterogeneous matrix, (D) EDS of particle in region 1 of pane B, (I) EDS of matrix region 2 of pane C.	S12
Figure S10. Representative elemental distribution in the IO_4^- treated **Ni-Cr** composite: (A) Representative SEM image of the **Ni-Cr** composite after being exposed to 10^{-1} M IO_4^- for 24 hours, (B, C, D) Ni, Cr and I mapping for region represented by pane A, (E) Representative SEM image of the **Ni-Cr** composite after being exposed to 10^{-1} M IO_4^- for 7 days, (F, G, H) Ni, Cr and I mapping for region represented by pane E.	S12
Figure S11. Representative elemental distribution in the IO_3^- treated **Ni-Cr** composite: (A) Representative SEM image of the **Ni-Cr** composite after being exposed to 10^{-1} M IO_3^- for 24 hours, (B, C, D) Ni, Cr and I mapping for region represented by pane A, (E) Representative SEM image of the **Ni-Cr** composite after being exposed to 10^{-1} M IO_3^- for 7 days, (F, G, H) Ni, Cr and I mapping for region represented by pane E.	S13
Figure S12. Representative elemental distribution in the I^- treated **Ni-Cr** composite: (A) Representative SEM image of the **Ni-Cr** composite after being exposed to 10^{-1} M I^- for 24 hours, (B, C, D) Ni, Cr and I mapping for region represented by pane A, (E) Representative SEM image of the **Ni-Cr** composite after being exposed to 10^{-1} M I^- for 7 days, (F, G, H) Ni, Cr and I mapping for region represented by pane E.	S13
References	S14

Table S1. Concentrations of the selected specified constituents in the groundwater collected from U.S. Department of Energy Hanford Site (200 area, well 299-W19-36). The complete groundwater composition is reported in reference 1.

Constituent	Concentration (µg/L)	Molarity (M)
Barium	113	8.23×10^{-07}
Calcium	122,000	3.04×10^{-03}
Chloride	181,000	5.11×10^{-03}
Total Cr	17.3	3.33×10^{-07}
Cr(VI)	0.05	9.62×10^{-10}
Magnesium	36,400	1.50×10^{-03}
Molybdenum	65.9	6.87×10^{-07}
Nitrate	317,000	5.11×10^{-03}
Potassium	7,010	1.79×10^{-04}
Sodium	118,000	5.13×10^{-03}
Sulfate	50,000	5.21×10^{-04}
Strontium	618	7.05×10^{-06}
Tin	216	1.82×10^{-06}
Alkalinity ($CaCO_3$)	116,000	1.16×10^{-03}
Uranium	174	7.31×10^{-07}
Iodine [a)]	8.6 ± 0.9	6.8×10^{-08}

[a)] Iodine concentration was measured in this work by ICP-MS analysis.

Table S2. Assignment of XPS peaks.

Assignment	Position (ev)
Cr $2p_{3/2}$ for Cr^{3+}	577.2[1]
Cr $2p_{3/2}$ for Cr^{6+}	579.2[2]
Cr $2p_{1/2}$ for Cr^{3+}	586.8[3]
Cr $2p_{1/2}$ for Cr^{6+}	588.7[3]
Co $2p_{3/2}$ for Co^{2+}	780.9[4]
Co $2p_{3/2}$ for Co^{3+}	779.8[5]
Co $2p_{3/2}$ for Co^{2+} satellite	782.6, 786.4[6]
Co $2p_{3/2}$ for Co^{3+} satellite	781.1[6]
Cl $2p_{3/2}$ for Cl^-	198.7[7]
Ni $2p_{3/2}$ for Ni^{2+}	855.7[6]
Ni $2p_{3/2}$ for Ni^{2+} satellites	857.7, 861.5, 866.5[6]
O 1s for $Cr(OH)_3$	531.7[8]
O 1s for Cr_2O_3	530.7[9]
O 1s for CrO_3	530.6[10]
O 1s for Co_3O_4	531.4[11]
O 1s for $Ni(OH)_2$	532.0[12]
I $3d_{5/2}$ for I^-	618.8[13]
I $3d_{5/2}$ for I_2	620.5[14]
I $3d_{5/2}$ for IO_3^-	623.9[15]
I $3d_{5/2}$ for IO_4^-	624.2[15]

Table S3. Elemental analysis of the marked regions in Figure S2 for the untreated **Co-Cr** and **Ni-Cr** composites obtained from EDS analyses showing the respective atomic percentages of the elements.

Co-Cr					
Region	**C**	**O**	**Cl**	**Cr**	**Co**
1	22.93	50.66	4.76	6.37	15.28
2	21.99	50.46	4.92	6.22	15.42
3	24	49.06	2.96	3.33	20.64
4	24.85	50.44	2.95	3.11	19.89
5	21.72	49.91	3.21	3.22	21.94
Ni-Cr					
Region	**C**	**O**	**Cr**	**Ni**	
6	32.21	45.44	6.40	15.95	
7	27.63	44.87	7.39	20.12	
8	24	49.06	3.30	20.67	

Table S4. Elemental analysis of the marked regions in Figure S4 for the IO_4^- treated **Co-Cr** composite obtained from EDS analyses showing the respective atomic percentages of the elements.

Region	**C**	**O**	**Cl**	**Cr**	**Co**	**I**
Exposure to IO_4^- for 24 hours						
1	24.63	45.37	0.63	8.48	20.88	0
2	25.08	48.24	2.63	3.42	20.64	0
3	14.6	49.52	1.74	10.33	19.94	3.85
Exposure to IO_4^- for 7 days						
4	21.63	49.15	0.63	3.48	23.88	1.23
5	23.08	38.24	0.63	12.42	20.64	4.99
6	22.08	39.24	0.63	12.37	20.71	4.97

Table S5. Elemental analysis of the marked regions in Figure S6 for the IO_3^- treated **Co-Cr** composite obtained from EDS analyses showing the respective atomic percentages of the elements.

Region	C	O	Cl	Cr	Co	I
Exposure to IO_3^- for 24 hours						
1	25.5	51.31	0.95	5.29	14.2	2.76
2	17.7	57.3	1.32	5.63	15.57	2.48
3	29.74	47.28	0.29	2.95	19.33	0.42
Exposure to IO_3^- for 7 days						
4	21.64	49.14	0.57	3.56	23.80	1.29
5	22.08	39.24	0.63	12.37	20.71	4.97
6	21.18	40.14	1.83	12.56	20.50	3.79

Table S6. Elemental analysis of the marked regions in Figure S8 for the I^- treated **Co-Cr** composite obtained from EDS analyses showing the respective atomic percentages of the elements.

Region	C	O	Cl	Cr	Co	I
Exposure to I^- for 24 hours						
1	22.26	56.22	1.44	5.84	13.64	0.61
2	23.89	52.61	1.17	5.7	16.09	0.55
3	22.89	50.58	0.71	3.01	22.56	0.26
4	19.62	55.48	0.82	3.98	21.99	0.31
Exposure to I^- for 7 days						
5	26.64	39.14	0.57	8.56	20.80	4.29
6	26.08	39.24	0.63	8.37	20.71	4.97

Table S7. Elemental analysis of the marked regions in Figure S10 for the IO_4^- treated **Ni-Cr** composite obtained from EDS analyses showing the respective atomic percentages of the elements.

Region	C	O	Cr	Ni	I
Exposure to IO_4^- for 24 hours					
1	21.26	56.44	6.46	16.84	1.15
2	13.61	62.58	3.22	21.59	1.63
3	19.84	51.68	6.61	16.80	1.20
Exposure to IO_4^- for 7 days					
4	22.57	50.43	3.02	16.89	7.08
5	27.86	45.14	3.13	16.87	6.99

Table S8. Elemental analysis of the marked regions in Figure S11 for the IO_3^- treated **Ni-Cr** composite obtained from EDS analyses showing the respective atomic percentages of the elements.

Region	C	O	Cr	Ni	I
Exposure to IO_3^- for 24 hours					
1	22.35	54.75	5.75	15.00	2.15
2	25.15	52.13	5.53	14.56	2.63
3	36.05	40.10	2.94	20.71	0.20
Exposure to IO_3^- for 7 days					
4	28.01	47.36	2.74	15.91	5.98
5	30.81	44.56	3.74	15.46	5.43
6	27.86	45.14	3.13	17.87	5.99

Table S9. Elemental analysis of the marked regions in Figure S12 for the I^- treated **Ni-Cr** composite obtained from EDS analyses showing the respective atomic percentages of the elements.

Region	C	O	Cr	Ni	I
Exposure to I^- for 24 hours					
1	16.79	57.01	3.90	21.40	0
2	17.48	59.74	5.83	16.35	0
3	22.89	45.81	3.14	23.69	0
Exposure to I^- for 7 days					
4	36.74	44.66	3.21	15.39	0
5	38.81	42.59	3.74	14.86	0

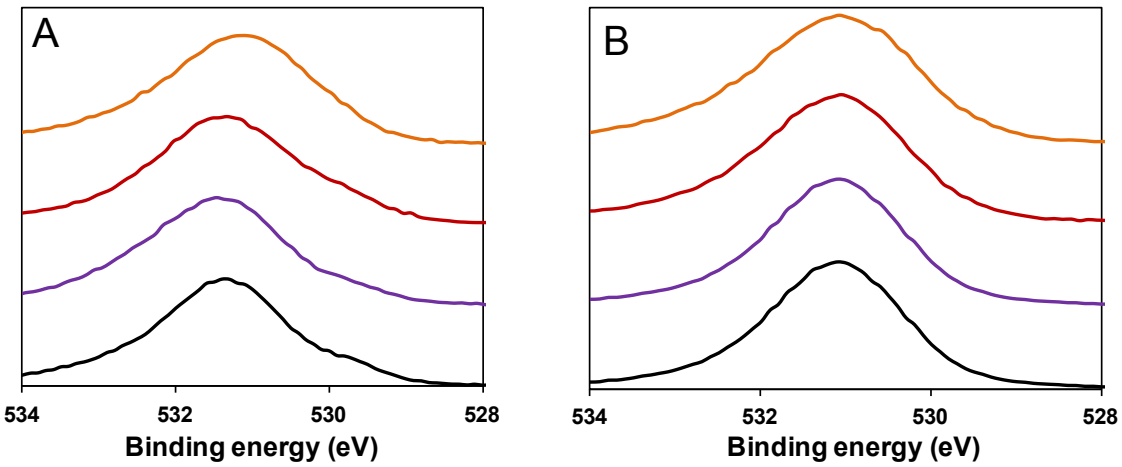

Figure S1. XPS patterns of (—) unexposed composites, and exposed to (—) 10^{-1} M I^-, (—) IO_3^- and (—) IO_4^- for 24 hours: O 1s region for (A) **Co-Cr**, (B) **Ni-Cr**.

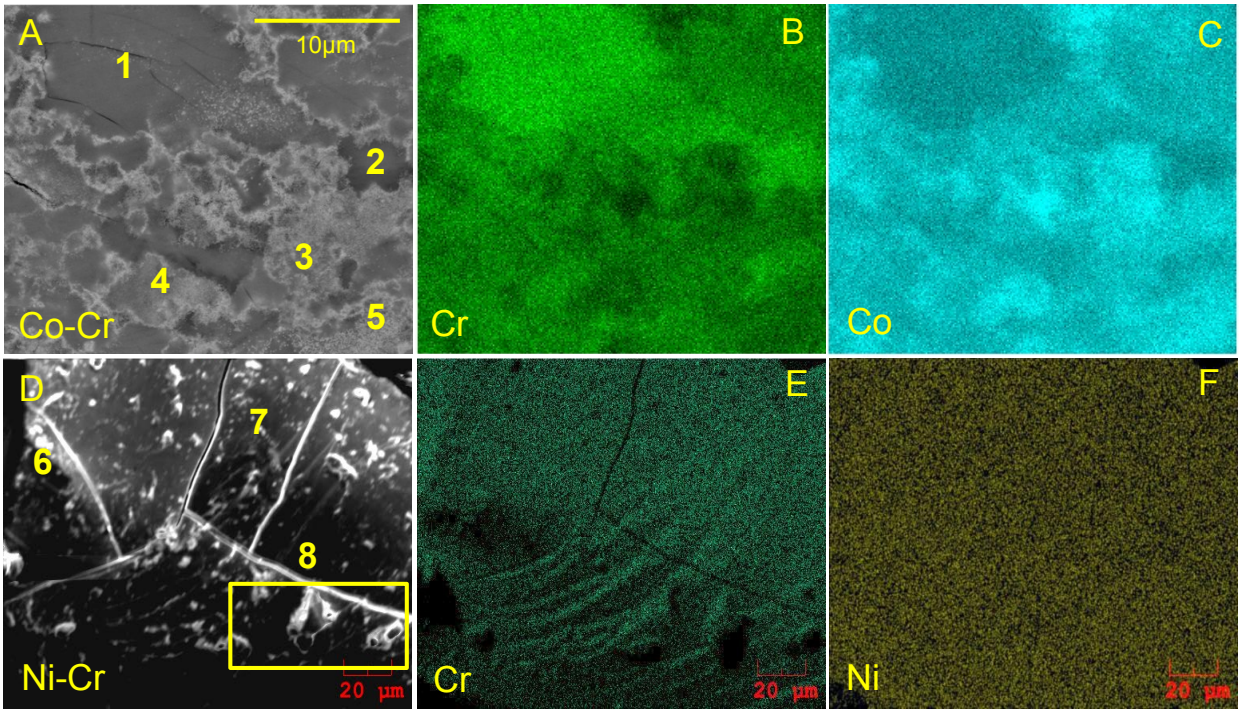

Figure S2. Representative elemental distribution in the untreated **M-Cr** composites: (A) Representative SEM of **Co-Cr** composite, (B) Cr mapping of the represented region (C) Co mapping for the represented region, (D) Representative SEM of **Ni-Cr** composite, (E) Cr mapping of the represented region (F) Co mapping for the represented region.

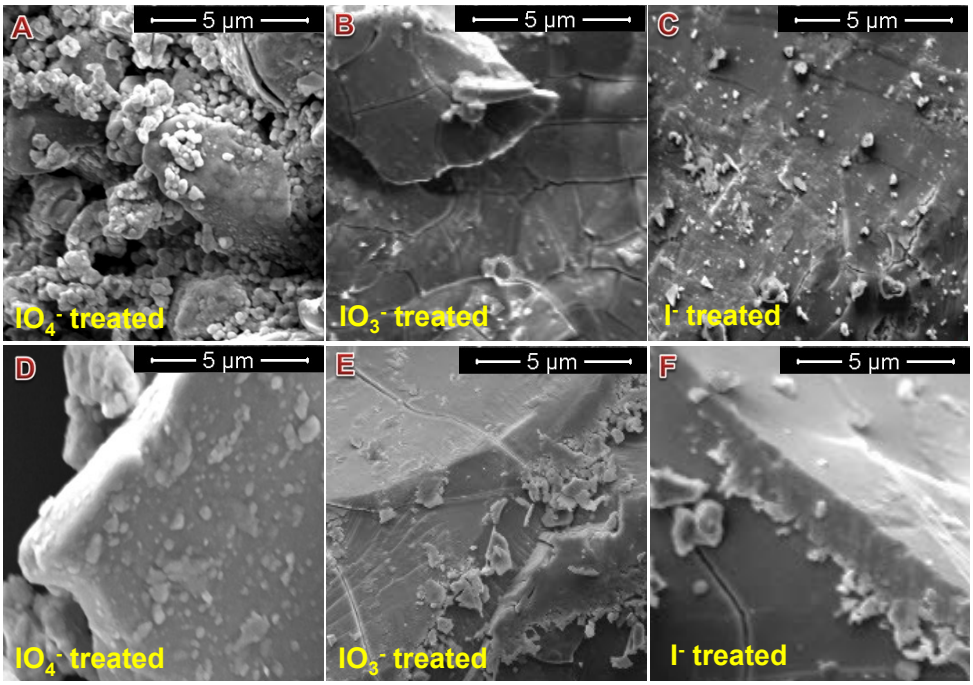

Figure S3. Representative SEM images of the composites: after 7 day exposure to aqueous solutions of anions: (A) **Co-Cr** exposed to 10^{-1} M IO_4^-, (B) **Co-Cr** exposed to 10^{-1} M IO_3^-, (C) **Co-Cr** exposed to 10^{-1} M I^-, (D) **Ni-Cr** exposed to 10^{-1} M IO_4^-, (E) **Ni-Cr** exposed to 10^{-1} M IO_3^-, (F) **Ni-Cr** exposed to 10^{-1} M I^-.

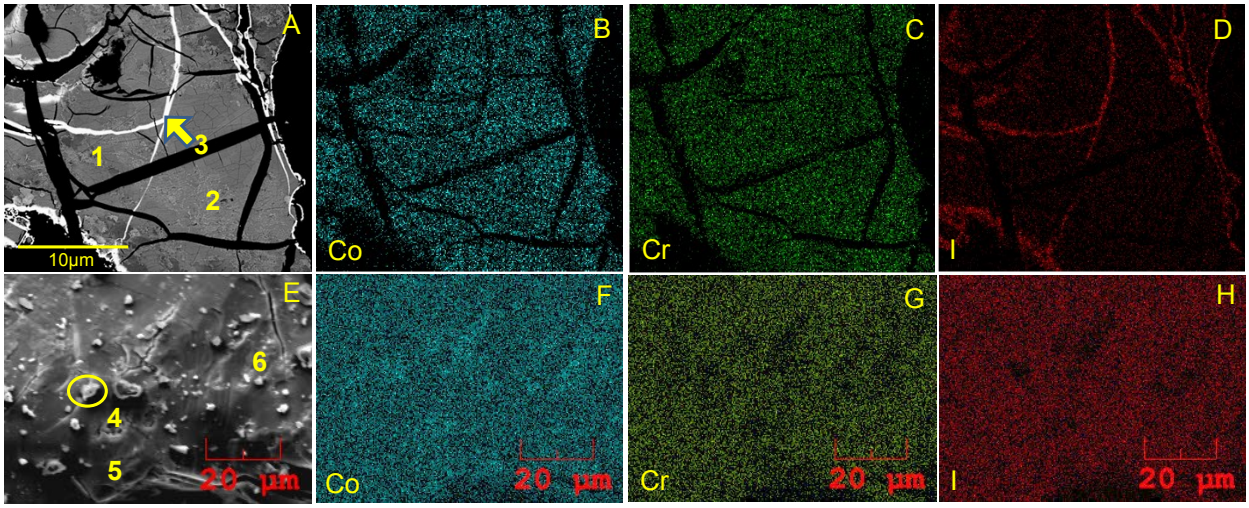

Figure S4. Representative elemental distribution in the IO_4^- treated **Co-Cr** composite: (A) Representative SEM image of the **Co-Cr** composite after being exposed to 10^{-1} M IO_4^- for 24 hours, (B, C, D) Co, Cr and I mapping for region represented by pane A, (E) Representative SEM image of the **Co-Cr** composite after being exposed to 10^{-1} M IO_4^- for 7 days, (F, G, H) Co, Cr and I mapping for region represented by pane E.

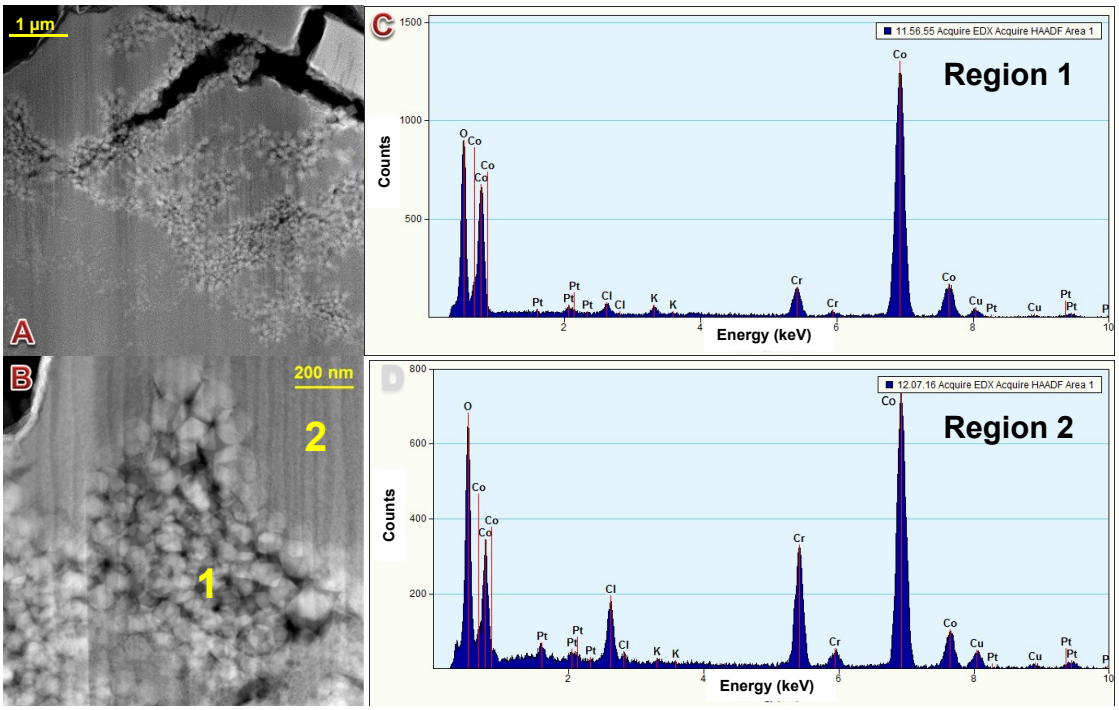

Figure S5. (A, B) Representative TEM image of **Co-Cr** composite after exposure to 10^{-1} M IO_4^- for 24 hours (C, D) the EDS analysis of regions marked 1 and 2 respectively in pane B.

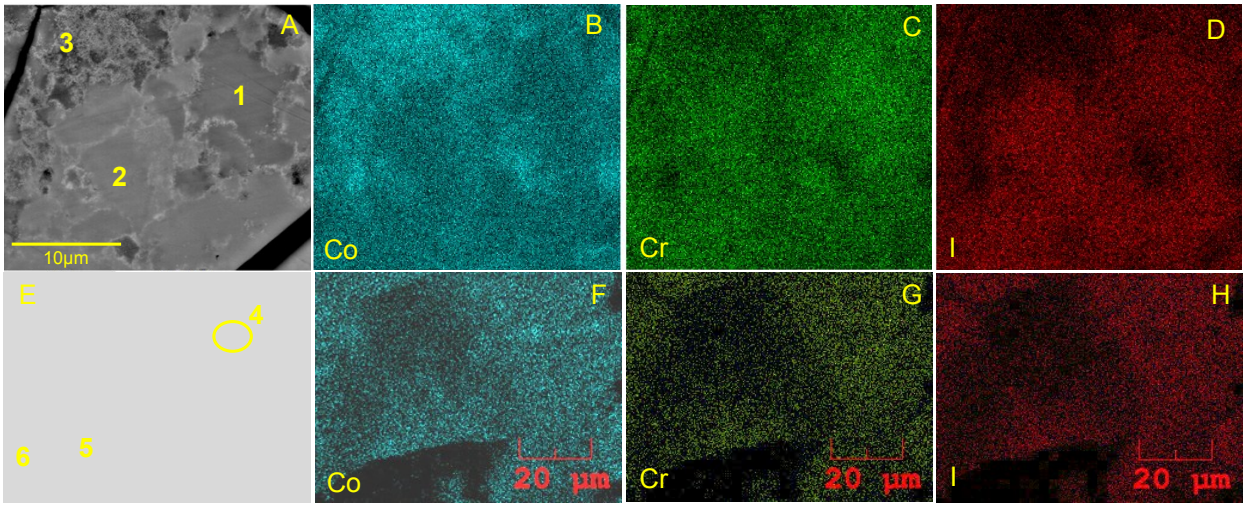

Figure S6. Representative elemental distribution in the IO_3^- treated **Co-Cr** composite: (A) Representative SEM image of the **Co-Cr** composite after being exposed to 10^{-1} M IO_4^- for 24 hours, (B, C, D) Co, Cr and I mapping for region represented by pane A, (E) Representative SEM image of the **Co-Cr** composite after being exposed to 10^{-1} M IO_3^- for 7 days, (F, G, H) Co, Cr and I mapping for region represented by pane E.

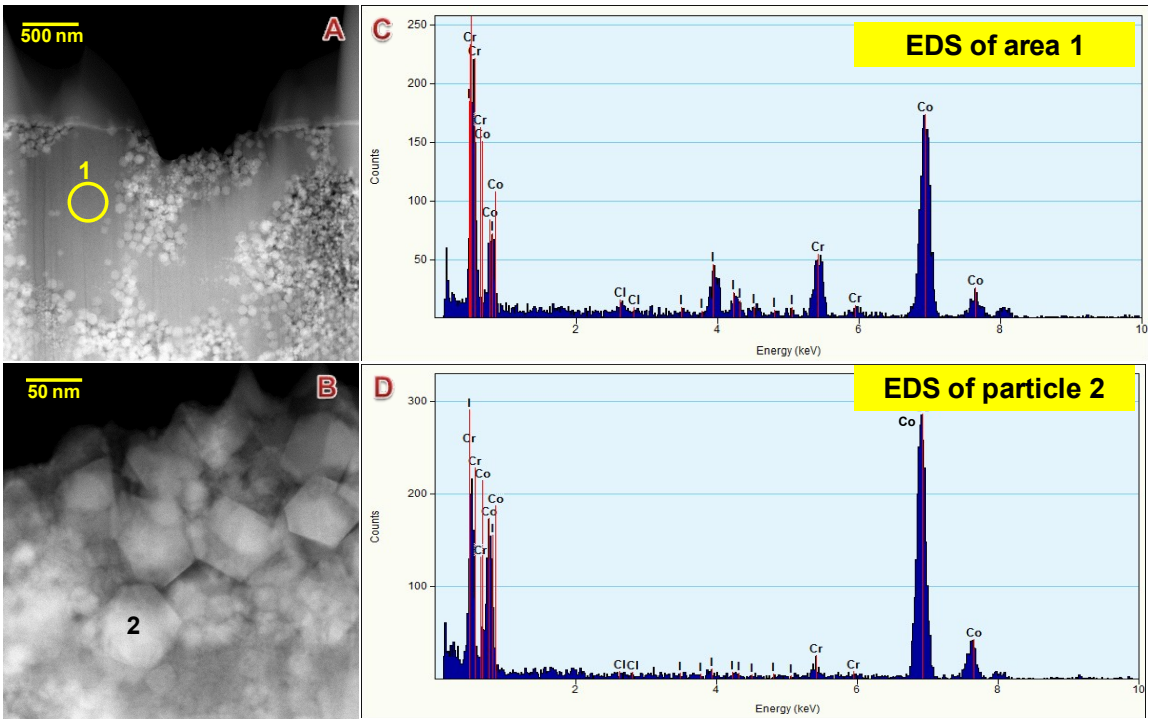

Figure S7. (A, B) Representative TEM image of **Co-Cr** composite after exposure to 10^{-1} M IO_3^- for 24 hours (C, D) the EDS analysis of regions marked 1 and 2 respectively in figure B.

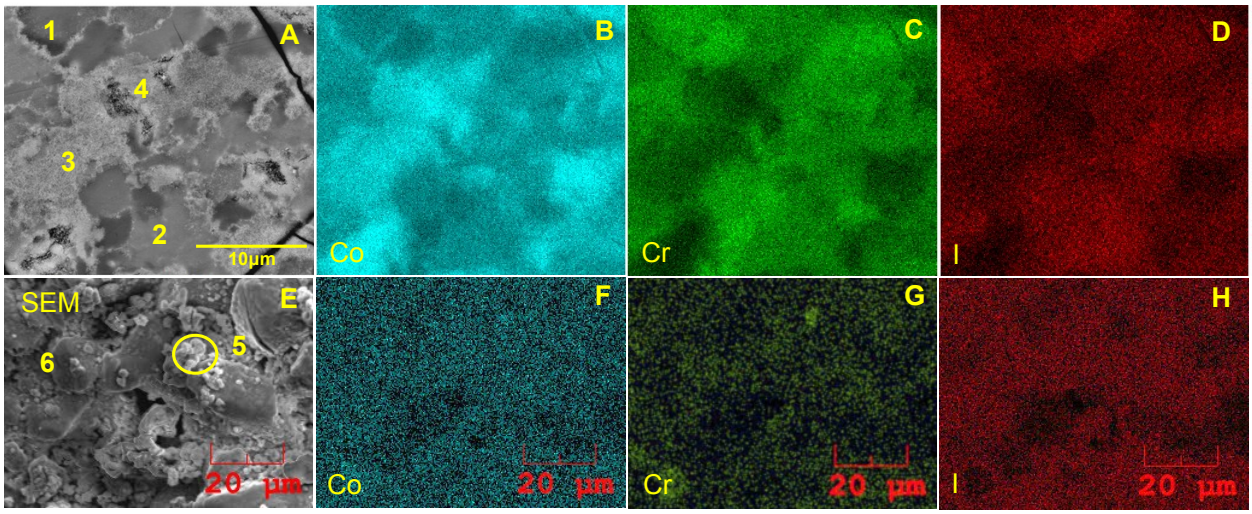

Figure S8. Representative elemental distribution in the I^- treated **Co-Cr** composite: (A) Representative SEM image of the **Co-Cr** composite after being exposed to 10^{-1} M I^- for 24 hours, (B, C, D) Co, Cr and I mapping for region represented by pane A, (E) Representative SEM image of the **Co-Cr** composite after being exposed to 10^{-1} M I^- for 7 days, (F, G, H) Co, Cr and I mapping for region represented by pane E.

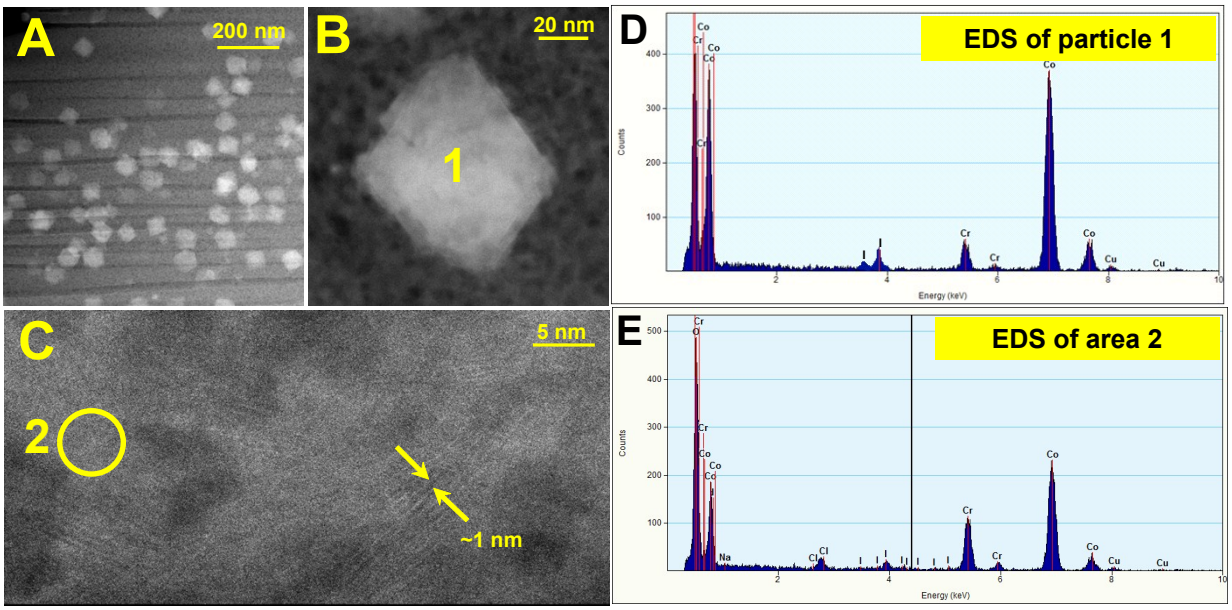

Figure S9. Co-Cr composite exposed to 10^{-1} M I^- for 24 hours: representative TEM images of the spinels (A) embedded in the heterogeneous matrix and (B) the magnified spinels, (C) representative TEM of the heterogeneous matrix, (D) EDS of particle in region 1 of pane B, (I) EDS of matrix region 2 of pane C.

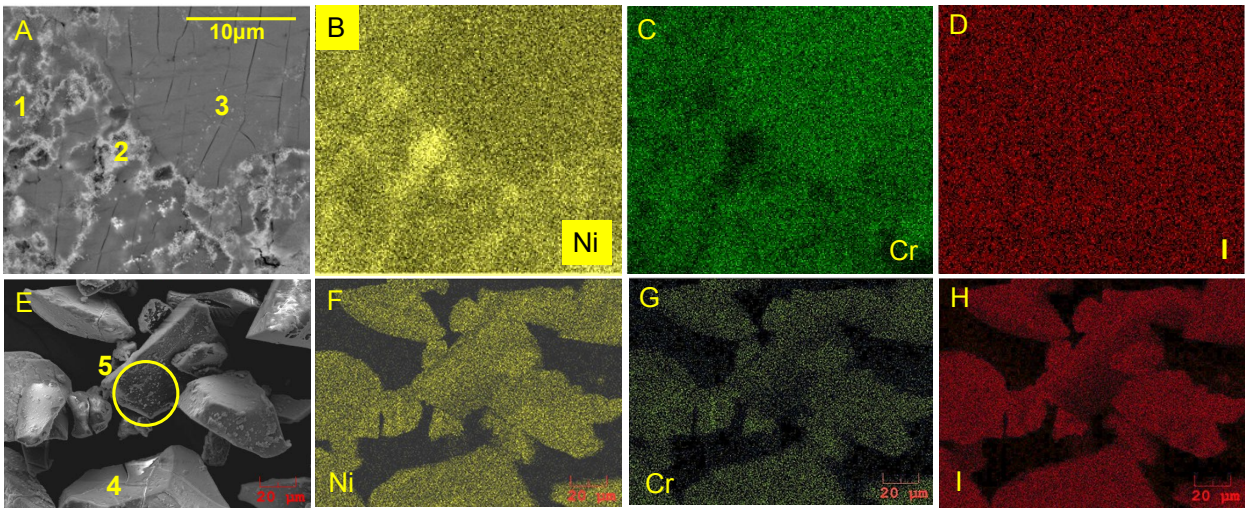

Figure S10. Representative elemental distribution in the IO_4^- treated **Ni-Cr** composite: (A) Representative SEM image of the **Ni-Cr** composite after being exposed to 10^{-1} M IO_4^- for 24 hours, (B, C, D) Ni, Cr and I mapping for region represented by pane A, (E) Representative SEM image of the **Ni-Cr** composite after being exposed to 10^{-1} M IO_4^- for 7 days, (F, G, H) Ni, Cr and I mapping for region represented by pane E.

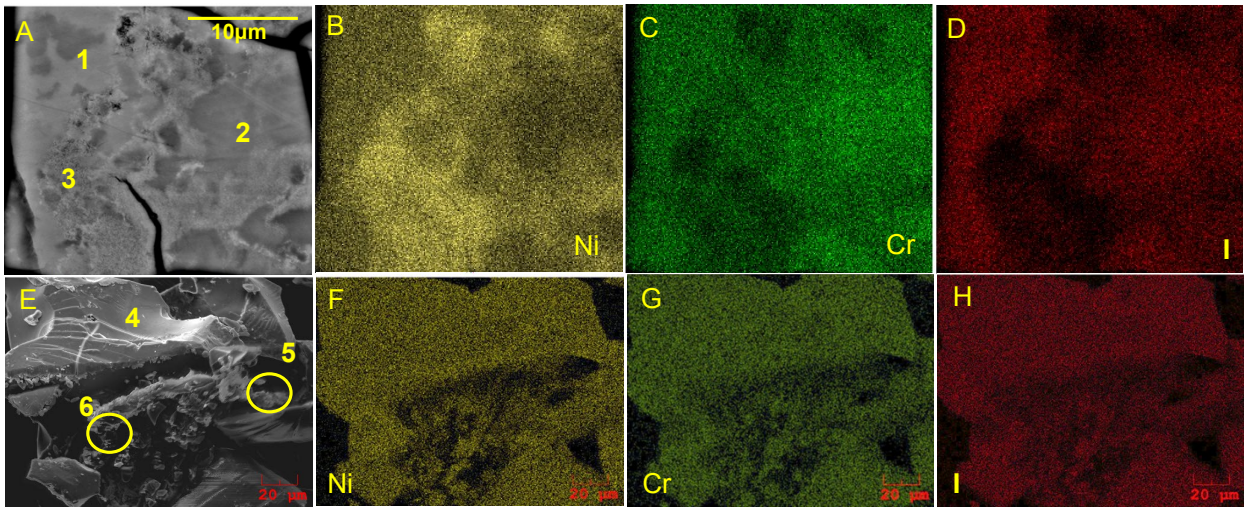

Figure S11. Representative elemental distribution in the IO_3^- treated **Ni-Cr** composite: (A) Representative SEM image of the **Ni-Cr** composite after being exposed to 10^{-1} M IO_3^- for 24 hours, (B, C, D) Ni, Cr and I mapping for region represented by pane A, (E) Representative SEM image of the **Ni-Cr** composite after being exposed to 10^{-1} M IO_3^- for 7 days, (F, G, H) Ni, Cr and I mapping for region represented by pane E.

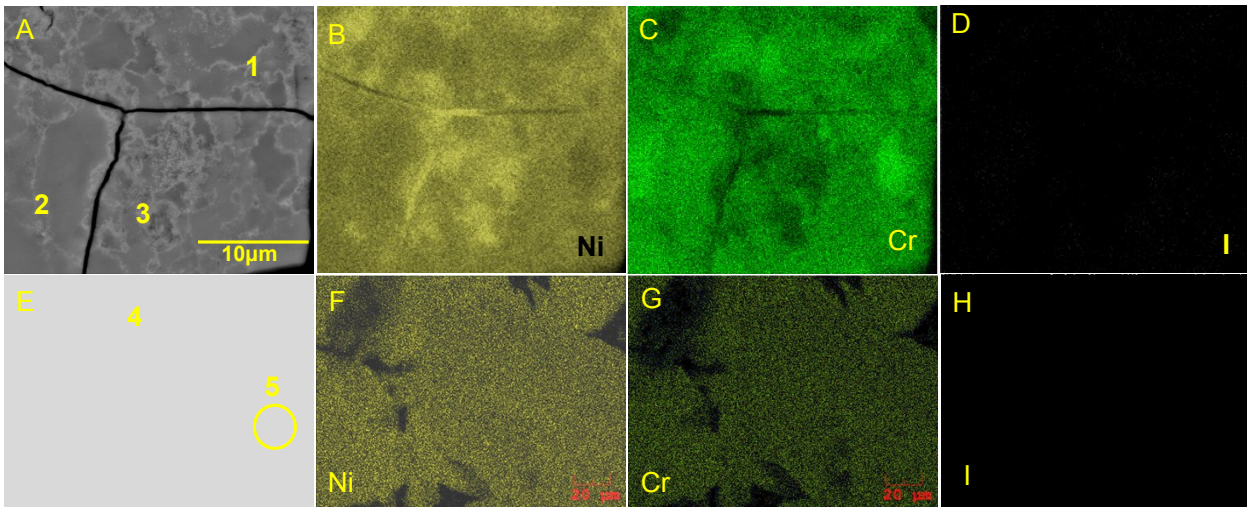

Figure S12. Representative elemental distribution in the I^- treated **Ni-Cr** composite: (A) Representative SEM image of the **Ni-Cr** composite after being exposed to 10^{-1} M I^- for 24 hours, (B, C, D) Ni, Cr and I mapping for region represented by pane A, (E) Representative SEM image of the **Ni-Cr** composite after being exposed to 10^{-1} M I^- for 7 days, (F, G, H) Ni, Cr and I mapping for region represented by pane E.

References:

(1) Paparazzo, E.; Severini, E.; Jimenezlopez, A.; Mairelestorres, P.; Oliverapastor, P.; Rodriguezcastellon, E.; Tomlinson, A. A. G. *J Mater Chem* **1992**, *2*, 1175.

(2) Merryfield, R.; Mcdaniel, M.; Parks, G. *J Catal* **1982**, *77*, 348.

(3) Desimoni, E.; Malitesta, C.; Zambonin, P. G.; Riviere, J. C. *Surf Interface Anal* **1988**, *13*, 173.

(4) Oku, M.; Hirokawa, K. *J Electron Spectrosc* **1976**, *8*, 475.

(5) Mcintyre, N. S.; Cook, M. G. *Anal Chem* **1975**, *47*, 2208.

(6) Biesinger, M. C.; Payne, B. P.; Grosvenor, A. P.; Lau, L. W. M.; Gerson, A. R.; Smart, R. S. *Appl Surf Sci* **2011**, *257*, 2717.

(7) Beard, B. C. *Surf. Sci. Spectra* **1993**, *2*, 91.

(8) Shuttleworth, D. *J Phys Chem-Us* **1980**, *84*, 1629.

(9) Marcus, P.; Grimal, J. M. *Corros Sci* **1992**, *33*, 805.

(10) Sleigh, C.; Pijpers, A. P.; Jaspers, A.; Coussens, B.; Meier, R. J. *J Electron Spectrosc* **1996**, *77*, 41.

(11) Tyuliev, G.; Angelov, S. *Appl Surf Sci* **1988**, *32*, 381.

(12) Liang, Y. L.; Sherwood, P. M. A.; Paul, D. K. *J Chem Soc Faraday T* **1994**, *90*, 1271.

(13) Morgan, W. E.; Stec, W. J.; Vanwazer, J. R. *J Am Chem Soc* **1973**, *95*, 751.

(14) Hsu, S. L.; Signorelli, A. J.; Pez, G. P.; Baughman, R. H. *J Chem Phys* **1978**, *69*, 106.

(15) Sherwood, P. M. A. *J Chem Soc Farad T 2* **1976**, *72*, 1805.